ISSN 1063-7710, Acoustical Physics, 2014, Vol. 60, No. 4, pp. 379–386. © Pleiades Publishing, Ltd., 2014.

CLASSICAL PROBLEMS
OF LINEAR ACOUSTICS AND WAVE THEORY

Fast Prediction of Scattered Sound Field Based on Fourier Diffraction Theory under Second-Order Born Approximation[1]

Peizhen Zhang[a, b] and Shuozhong Wang[a]

[a] *School of Communication and Information Engineering, Shanghai University, Shanghai, 200072 China*
e-mail: shuowang@shu.edu.cn

[b] *School of Information, Guangdong Ocean University, Zhanjiang, 524088 China*
e-mail: zpzhen7242@163.com

Received September 21, 2013

Abstract—The directional pattern of sound waves scattered from an object insonified by a plane wave can be efficiently predicted using the Fourier diffraction theorem (FDT). This is achieved by sampling a circle in the discrete Fourier transform of the object/medium distribution. However, the FDT-based approach under the first-order Born approximation is only applicable to weak scattering. To improve the prediction accuracy and expand the method's scope of applications, we introduce a second-order correction term to the solution, which is obtained by taking the first-order scattered waves as secondary incident sources, and calculate the "scattering" in the same way as in the first-order FDT-based approach. Adding the resulting correction term to the directional pattern based on the first-order Born approximation, the second-order prediction is obtained. Numerical results show that the proposed method can provide improved directional patterns of the scattered waves, and the range of applicability is significantly expanded.

Keywords: sound scattering, directional pattern, fast prediction, Fourier diffraction theorem (FDT), Born approximation

DOI: 10.1134/S1063771014040198

1. INTRODUCTION

When an incident sound wave impinges an object, it is reflected and scattered. Prediction of the scattered sound field, given the properties of the scattering object insonified by a known incident wave, is an important issue both in theoretical studies and in applications [1]. In principle, the scattered sound field may be computed by solving the governing wave equation. However, rigorous analytical solution of the wave equation is hardly possible, except for a few ideal cases such as liquid spheres [2] and simple cylinders [3]. Numerical approaches are often sought to treat various practical problems.

Frequently used numerical approaches include the finite element method/boundary element method (FEM/BEM) [4, 5] and the finite-difference time-domain method (FDTD) [6, 7]. These methods divide the field into grids and generally mean heavy computation loads. Instead of FEM and FDTD, it is possible to use the Fourier diffraction theorem (FDT) to treat the scattering problem in a different perspective from its conventional use for solving inverse problems such as diffraction tomography [8]. A fast algorithm has been developed using the FDT framework, in which the first-order Born approximation is used to solve the Helmholtz equation [9, 10]. The first-order approximation limits the usage of the algorithm to weak scattering cases in which the acoustic impedance of the scattering object is not significantly different from that of the surrounding water. For example, the first-order method is applicable to scattering from squid, jellyfish, and various zooplanktons in the ocean.

A series of research have been done to improve accuracy of scattering prediction and expand the scope of applications. For example, Iwata et al. improve the accuracy by taking into consideration the difference in density and sound speed of the scattering object [11]. Jones et al. introduce the distorted wave Born approximation (DWBA) to treat squid. They model the squid as a cylindrical shell filled with liquid [12]. Saha et al. improve the Born approximation by correcting the wave number inside the object according to its sound speed [13]. The second-order Born approximation has been considered in treating an inverse problem, i.e., acoustical tomography, by Lu et al. They apply a first-order integral operator to the angular spectrum of the scattered wave, or a second-order integral operator to that of the incident wave, to improve tomographic resolution [14].

In this paper, we show that, with the FDT-based framework for fast prediction of scattering fields, the second-order Born approximation can be imple-

[1] The article is published in the original.

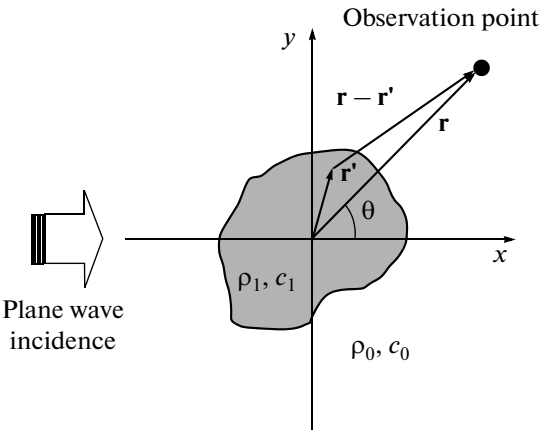

Fig. 1. Two-dimensional sound scattering with the direction of incidence $\varphi = 0°$.

mented. Following a brief description of the FDT-based approach, we propose a method to incorporate the second approximation into the algorithm, and show effectiveness of the method by numerical computation. Shear waves are not considered in the present work, and therefore the scattering objects are of the fluid nature.

2. FOURIER DIFFRACTION THEOREM AND FIRST BORN APPROXIMATION IN SOUND SCATTERING PREDICTION

Consider a 2D scattering problem in which an infinitely long cylinder with an arbitrarily shaped cross-section immersed in water is insonified by a plane sound wave propagating perpendicularly to the cylinder's axis, see Fig. 1. Assume that densities of the scattering object and the water are ρ_1 and ρ_0, and their sound velocities c_1 and c_0, respectively. Let φ and θ be the angles of incidence and scattering, respectively. In Fig. 1, the incidence is in the positive x direction, i.e., $\varphi = 0$. The vector $\mathbf{r} = (x, y)$ represents the field location, and $\mathbf{r}' = (x', y')$ is on the source of the scattered waves, i.e., on the scattering object.

Denote the distribution of acoustical properties of the object and the surrounding medium as $o(\mathbf{r})$. If the object is made of a homogeneous material, $o(\mathbf{r})$ may be viewed as a binary image with its values equal to $[c_0^2/c_1^2(\mathbf{r}) - 1]$ inside the object, and zero in the water. In case of weak scattering, the scattered sound field can be obtained by solving the Helmholtz equation under the first-order Born approximation [15]:

$$p_s(\mathbf{r}) \approx \int o(\mathbf{r}')p_i(\mathbf{r}')g(\mathbf{r}|\mathbf{r}')d\mathbf{r}', \quad |p_s| \ll |p_i|. \tag{1}$$

Note that the total field $p = p_s + p_i$ in the integrand is replaced with the incident field p_i. If the incident sound wave is in a direction that forms an angle φ with the x axis,

$$p_i(\mathbf{r}) = \exp[jk_0(x\cos\varphi + y\sin\varphi)]. \tag{2}$$

Without loss of generality, we will assume $\varphi = 0$ in the following discussion:

$$p_i(\mathbf{r}) = \exp(jk_0x). \tag{3}$$

Taking into account the different wave number and density inside the scattering object, the first-order solution of the scattered wave is [16]

$$p_s(\mathbf{r}) = \left(\int k_0^2\gamma_\kappa o(\mathbf{r}')p_i(\mathbf{r}')g(\mathbf{r}|\mathbf{r}') + \gamma_\rho o\nabla p_i(\mathbf{r}')\nabla g(\mathbf{r}|\mathbf{r}')\right)d\mathbf{r}'. \tag{4}$$

The constants γ_κ and γ_ρ are related to the contrast of the density ρ and compressibility $\kappa = 1/(\rho c^2)$ inside and outside the scattering object:

$$\gamma_\rho = \frac{\rho_1 - \rho_0}{\rho_1\mu}, \quad \gamma_\kappa = \frac{\kappa_1 - \kappa_0}{\kappa_1}. \tag{5}$$

Both γ_κ and γ_ρ are zero outside the object.

The Green's function $g(\mathbf{r}|\mathbf{r}')$ in the expressions is a zero-order Hankel function of the first kind, whose far-field approximation can be expressed as

$$g(\mathbf{r}|\mathbf{r}') = \sqrt{\frac{2}{\pi r}}\exp[-jk_0(x'\cos\theta + y'\sin\theta)] \times \exp\left(jk_0r - j\frac{\pi}{4}\right), \tag{6}$$

where $\mathbf{r} = \{r, \theta\}$.

Substituting the incident wave (3) and the Green's function (6) into (4), the far-field scattered sound pressure can be written as

$$p_s(r, \theta) = k_0^2 f^{[1]}(\theta)\sqrt{\frac{2}{\pi r}}\exp\left(jk_0r - j\frac{\pi}{4}\right), \tag{7}$$

where $f^{[1]}(\theta)$ is the directional pattern of the first-order scattered sound field:

$$f^{[1]}(\theta) = (\gamma_\kappa + \gamma_\rho\cos\theta)O(k_0\cos\theta - k_0, k_0\sin\theta). \tag{8}$$

Here $O(\cdot)$ is 2D Fourier transform of the function $o(\mathbf{r})$. Equations (7) and (8) indicate that the scattered sound field can be obtained by sampling the Fourier transform of the object's cross-sectional image on a circle centered at $(-k_0, 0)$ and with a radius k_0. If we sample the circle at an angular interval of 1°, we can obtain the following vector of the first-order directional pattern:

$$\mathbf{f}^{[1]} = [f^{[1]}(0)f^{[1]}(1)\cdots f^{[1]}(d)\cdots f^{[1]}(359)]^T, \tag{9}$$

where

$$f^{[1]}(d) = \left(\gamma_\kappa + \gamma_\rho\cos\frac{2\pi d}{360}\right) \times O\left(k_0\cos\frac{2\pi d}{360} - k_0, k_0\sin\frac{2\pi d}{360}\right), \quad d = 0, 1, \ldots, 359. \tag{10}$$

The above discussion forms the basis of a fast algorithm for scattered sound prediction under the first-order Born approximation. The sampling locus is shown in Fig. 2 by the solid circle in the Fourier trans-

form domain. If the incident angle φ is not zero, the sampling circle will rotate around the origin. For example, the three dashed circles in the figure correspond to $\varphi = \pi/2$, π and $3\pi/2$, respectively.

3. SECOND-ORDER BORN APPROXIMATION IN THE FDT FRAMEWORK

In Eq. (1), the scattered sound pressure is omitted in the integrand to give the first approximation. The omission will cause a noticeable error when the object's acoustic impedance gradually departs from that of the water. Kak [15] suggests improving accuracy by adding the contribution of the scattered sound of the first approximation to obtain the second approximation:

$$p_s^{(2)}(\mathbf{r}) = \int o(\mathbf{r}')[p_i(\mathbf{r}') + p_s^{(1)}(\mathbf{r}')]g(\mathbf{r}|\mathbf{r}')d\mathbf{r}'. \quad (11)$$

The superscripts in the parentheses represent the orders of approximation. This can further be generalized to produce the $(n+1)$th approximation:

$$p_s^{(n+1)}(\mathbf{r}) = \int o(\mathbf{r}')[p_i(\mathbf{r}') + p_s^{(n)}(\mathbf{r}')]g(\mathbf{r}|\mathbf{r}')d\mathbf{r}', \quad n = 1, 2, \ldots . \quad (12)$$

Alternatively, by expressing the scattering contributions of various orders separately,

$$p_s^{[n+1]}(\mathbf{r}) = \int o(\mathbf{r}')p_s^{[n]}(\mathbf{r}')g(\mathbf{r}|\mathbf{r}')d\mathbf{r}', \quad n = 1, 2, \ldots, \quad (13)$$

where $p_s^{[1]}(\mathbf{r})$ is calculated using Eq. (4). The pressure with a superscript $[n]$ in square brackets ($n > 1$) represents an increment of the scattered wave of the nth order, rather than the entire scattered field. Thus,

$$p_s(\mathbf{r}) = \sum_{n=1}^{\infty} p_s^{[n]}(\mathbf{r}). \quad (14)$$

The interpretation of Eq. (13) is based on the Huygens principle: each point in the object produces a scattered field proportional to the scattering potential at the site of the scatterer.

The above proposition is attractive, but an algorithm for implementation is not available. We now show that, in the framework of the Fourier diffraction theorem approach and using the corresponding fast algorithm, the second order approximation can easily be implemented to achieve improved accuracy.

It is observed from (13) that the second-order approximation is achieved by adding to the first-order approximation $p_s^{[1]}(\mathbf{r})$ an incremental, or correctional, term $p_s^{[2]}(\mathbf{r})$, which can be calculated in the same way as described in Section 2 as if $p_s^{[1]}(\mathbf{r})$ is a secondary incident wave. Note that, unlike $p_i(\mathbf{r})$, the first-order scattering waves are in all directions and with the strength proportional to the angular pattern $f^{[1]}(\theta)$.

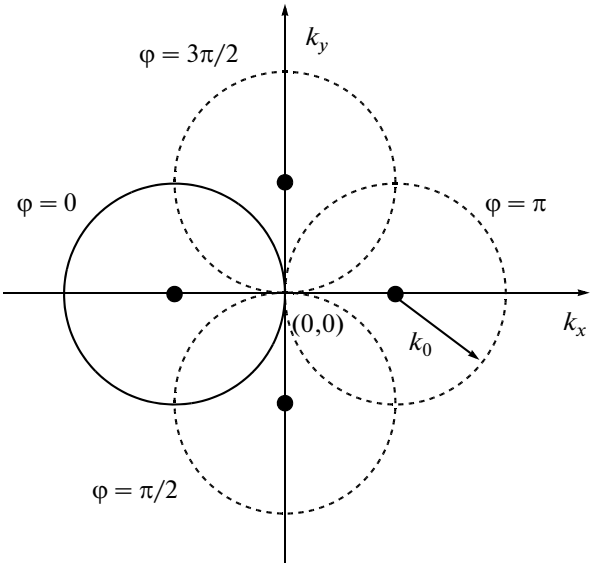

Fig. 2. Sampling circles in the Fourier domain with the incident angle being 0, $\pi/2$, π and $3\pi/2$.

Substitute $p_s^{[1]}(\mathbf{r})$ given by (4) into (13) with $n = 1$, and integrate over the entire field to obtain the second-order increment to the first-order scattered wave, or the correction term of the second order:

$$p_s^{[2]}(\mathbf{r}) = \int o(\mathbf{r}')p_s^{[1]}(\mathbf{r}')g(\mathbf{r}|\mathbf{r}')d\mathbf{r}'$$
$$= \int o(\mathbf{r}')\{\int [k_0^2\gamma_\kappa o(\mathbf{r}'')p_i(\mathbf{r}'')g(\mathbf{r}'|\mathbf{r}'') + \gamma_\rho o(\mathbf{r}'')\nabla p_i(\mathbf{r}'')\cdot\nabla g(\mathbf{r}'|\mathbf{r}'')]d\mathbf{r}''\}g(\mathbf{r}|\mathbf{r}')d\mathbf{r}'. \quad (15)$$

Here the first-order scattered waves act as the incidence of the second order.

Since the scattered waves originate from the object, according to [12] and [17], the exponential term of the secondary incident waves that generate the higher-order scattering is $\exp[jk_0(1+\alpha)x] = \exp(jk_1x)$ rather than $\exp(jk_0x)$, where α is deviation of the object material's refraction index with respect to water,

$$\alpha = \frac{c_0 - c_1}{c_1} = \frac{\Delta c}{c_1}. \quad (16)$$

Thus the second-order increment to the first-order scattered wave $p_s^{[2]}(\mathbf{r})$ can be obtained. To find the directional pattern $f^{[2]}(\theta^{[2]})$ of $p_s^{[2]}(\mathbf{r})$, we first calculate the contribution of the first-order scattered wave in the direction of $\theta^{[1]}$ and within an angular interval $\delta\theta^{[1]}$:

$$\delta f^{[2]}(\theta^{[1]}, \theta^{[2]}) = g(\theta^{[1]}, \theta^{[2]})h(\theta^{[1]})\delta\theta^{[1]}, \quad (17)$$

where

$$g(\theta^{[1]}, \theta^{[2]}) = (k_0^2\gamma_\kappa + \gamma_\rho k_1^2\cos\theta^{[1]}) \times O(k_1\cos\theta^{[2]} - k_1\cos\theta^{[1]}, k_1\sin\theta^{[2]} - k_1\sin\theta^{[1]}) \quad (18)$$

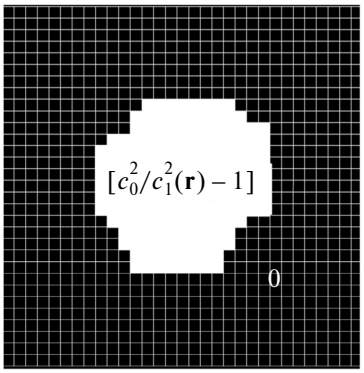

Fig. 3. Image representing the object and its surrounding medium.

and

$$h(\theta^{[1]}) = O(k_1\cos\theta^{[1]} - k_1, k_1\sin\theta^{[1]}). \quad (19)$$

For the derivation of the directional pattern of the second-order correction, see Appendix A.

Let $\delta\theta^{[1]} = 2\pi/M$, and sum up over all directions $\theta^{[1]}$ to get the second-order correction to the first-order result in any scattering direction:

$$f^{[2]}(\theta) = \sum_{m=0}^{M-1}\delta f^{[2]}\left(\frac{2\pi m}{M}, \theta\right) = \frac{2\pi}{M}\sum_{m=0}^{M-1} g\left(\frac{2\pi m}{M}, \theta\right)h\left(\frac{2\pi m}{M}\right). \quad (20)$$

Here we have omitted the superscript of θ that represents the direction of the second-order scattering. The entire directional pattern of the second-order correction term can be obtained by calculating $f^{[2]}(\theta)$ of different scattering angles θ and then summing them up. Considering M directions, the directional pattern can be evaluated in the following matrix form:

$$\mathbf{f}^{[2]} = \mathbf{G}\mathbf{h}, \quad (21)$$

where $\mathbf{h}$ is a column vector:

$$\mathbf{h} = \frac{2\pi}{M}\left[h(0)\ h\left(\frac{2\pi}{N}\right)\ \cdots\ h\left(\frac{2\pi(M-1)}{M}\right)\right]^T. \quad (22)$$

Considering the second-order term in an angular interval of 1° as in the first-order case, $\mathbf{G}$ is a 360-by-M matrix:

$$\mathbf{G} = \left[\mathbf{g}_0\ \mathbf{g}_1\ \cdots\ \mathbf{g}_m\ \cdots\ \mathbf{g}_{M-1}\right], \quad (23)$$

where $\mathbf{g}_m$ are column vectors:

$$\boldsymbol{g}_m = \left[g\left(\frac{2\pi m}{M}, 0\right)\ g\left(\frac{2\pi m}{M}, \frac{2\pi}{360}\right)\ \cdots\ g\left(\frac{2\pi m}{M}, \frac{2\pi d}{360}\right)\ \cdots\ g\left(\frac{2\pi m}{M}, \frac{2\pi\times 359}{360}\right)\right]^T,\ m = 0, 1, \ldots, M-1. \quad (24)$$

Vector $\mathbf{g}_m$ represents the contribution of the first-order scattering in the mth sector with an angular width $\delta\theta = 2\pi/M$.

Similar to (9), $\mathbf{f}^{[2]}$ is a 360-element vector:

$$\mathbf{f}^{[2]} = \left[f^{[2]}(0)\ f^{[2]}(1)\ \cdots\ f^{[2]}(d)\ \cdots\ f^{[2]}(359)\right]^T. \quad (25)$$

Thus, the final directional pattern of the scattered sound field under the second-order Born approximation is obtained:

$$\mathbf{f} = \mathbf{f}^{[1]} + \mathbf{f}^{[2]}. \quad (26)$$

4. ALGORITHM FOR IMPLEMENTATION

According to the foregoing discussion, an algorithm of fast scattering prediction based on the Fourier diffraction theorem and second-order Born approximation, given the wave number of the incident plane wave k_0 and the scattering object, can be summarized as follows.

(1) Define a rectangular area enclosing the scattering object, and divide it into grids with the grid size sufficiently smaller than the wavelength, say, less than λ/10. The rectangular area including the object and the surrounding medium (water) can be viewed as a digital image $o(i, j)$ whose pixel values equal $[c_0^2/c_1^2(\mathbf{r})-1]$ inside the object and 0 outside, see Fig. 3.

(2) Calculate the two-dimensional FFT of the image to give its spectrum $O(u, v)$. The jaggy edges of the object due to coarse sampling in the space domain introduce artifacts into the transform domain, seriously affecting the accuracy of scattering prediction. A method of repeated interpolation-smoothing-decimation operations [18] is used to reduce jaggedness and improve quality of the spectrum.

(3) The first-order scattering solution $\mathbf{f}^{[1]}$ is obtained by sampling the solid circle in the transform domain, as shown in Fig. 2, at an angular interval of 1°.

(4) Divide the first-order scattering solution into M sectors, each having an angular width of $2\pi/M$.

(5) Find the contribution of each sector of the first-order scattering to the second-order correction term. For the mth sector, as the angle of incidence is $2\pi m/M$, the sampling circle is centered at $(-k_1\cos 2\pi m/M, -k_1\sin 2\pi m/M)$, with radius k_1, as shown in Fig. 4. Sample a total of M such circles at 1° intervals, each producing a 360-element vector as a component of $\mathbf{f}^{[2]}$.

(6) Sum up the M contributions to produce a vector $\mathbf{f}^{[2]}$, which is the second-order correction to the scattering.

(7) Obtain the directional pattern of the scattered sound under the second-order Born approximation according to (26).

5. NUMERICAL COMPUTATION RESULTS

We consider an infinitely long circular cylinder, and a plane sound wave incident in a direction perpendicular to the axis. Parameters used in the numerical computation are listed in table. Two groups of the cylinder's material are studied: softer than water and harder than water, with the ratios between the cylinder material's density and that of water, $D = \rho_1/\rho_0$, and between the sound speeds, $S = c_1/c_0$, ranging from 0.85 to 0.99, and from 1.01 to 1.20, respectively. Therefore, the ρc ratio under consideration ranges from 0.72 to 1.44.

Figures 5 and 6 give the computation results. They are directional patterns of scattered sound pressure normalized to 1 for $\theta = 0$, with both D and S being 0.85, 0.90 and 0.99 for softer materials, and 1.01, 1.10 and 1.20 for harder materials, respectively. The vertical axes are drawn to the logarithmic scale. For each material, three k_0R values, 3, 5 and 10 are used. In the plots, the thick lines are the second-order Born approximation results, which are compared with the first-order approximation in thin lines, and the rigorous analytical results in dashed lines. The analytical results are obtained using the solutions given in [3].

It is observed from the plots that, when the acoustic impedance of the cylinder is near that of water, both the first- and second-order approximation results are close to the analytical solution. When the acoustic impedance of the cylinder departs from that of water, errors of the first-order approximation become large, even intolerable, as the first-order approximation is only applicable to weak scattering, while the second-order approximation always provides better results.

6. CONCLUSIONS

By using the Fourier diffraction theorem in a reversed manner with respect to diffraction tomography, we can solve a forward problem in acoustics: prediction of the scattered sound field from a known incident wave and the geometry and physical properties of the scattering object. The reversed application of FDT offers a significant advantage in computation efficiency compared to the popular lattice-based numerical methods, typically FEM/BEM and FDTD. As no space-demanding grids and time-consuming iterations are needed, and fast Fourier transform can be used, substantial reduction in the computation burden is achieved. This makes the FDT-based framework potentially suitable for many applications.

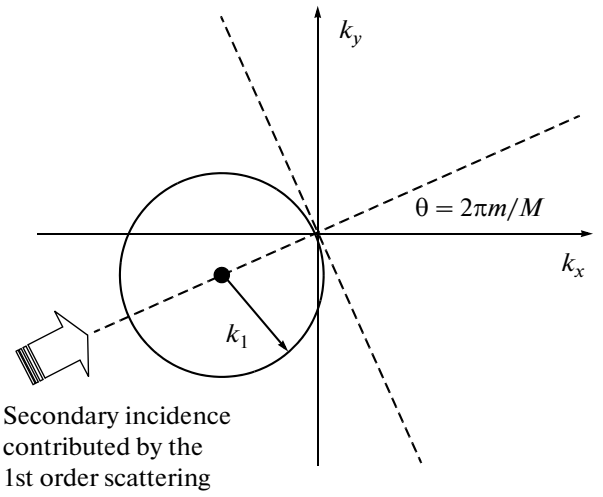

Fig. 4. Sampling circle for the second-order correction component contributed by the mth first-order scattering, with the center at $(-k_1\cos 2\pi m/M, -k_1\sin 2\pi m/M)$.

Under the first-order Born approximation, however, the FDT-based method can only provide usable results for scattering objects with acoustical impedance very close to that of the surrounding medium. To improve accuracy and overcome the weak scattering limitation, we propose to improve the FDT-based method by considering the second-order Born approximation. We have shown that by treating the first-order scattered waves as secondary

Parameters of the scattering cylinder and the incident sound

Item	Symbol	Unit	Value
Frequency of sound	f_0	Hz	1500
Sound speed in water	c_0	m/s	1500
Wave number	$k_0 = 2\pi f_0/c_0$	rad/m	6.28
Density of water	ρ_0	kg/m^3	1027
Size of sampling grid	δ	m	0.1
Side of the square area	a	m	12.8
k_0R where R is radius of cylinder	$k_0R = 2\pi R/\lambda$	–	3–10
Ratio of densities between cylinder and water	D	–	0.85–1.20
Ratio of sound speed between cylinder and water	S	–	0.85–1.20

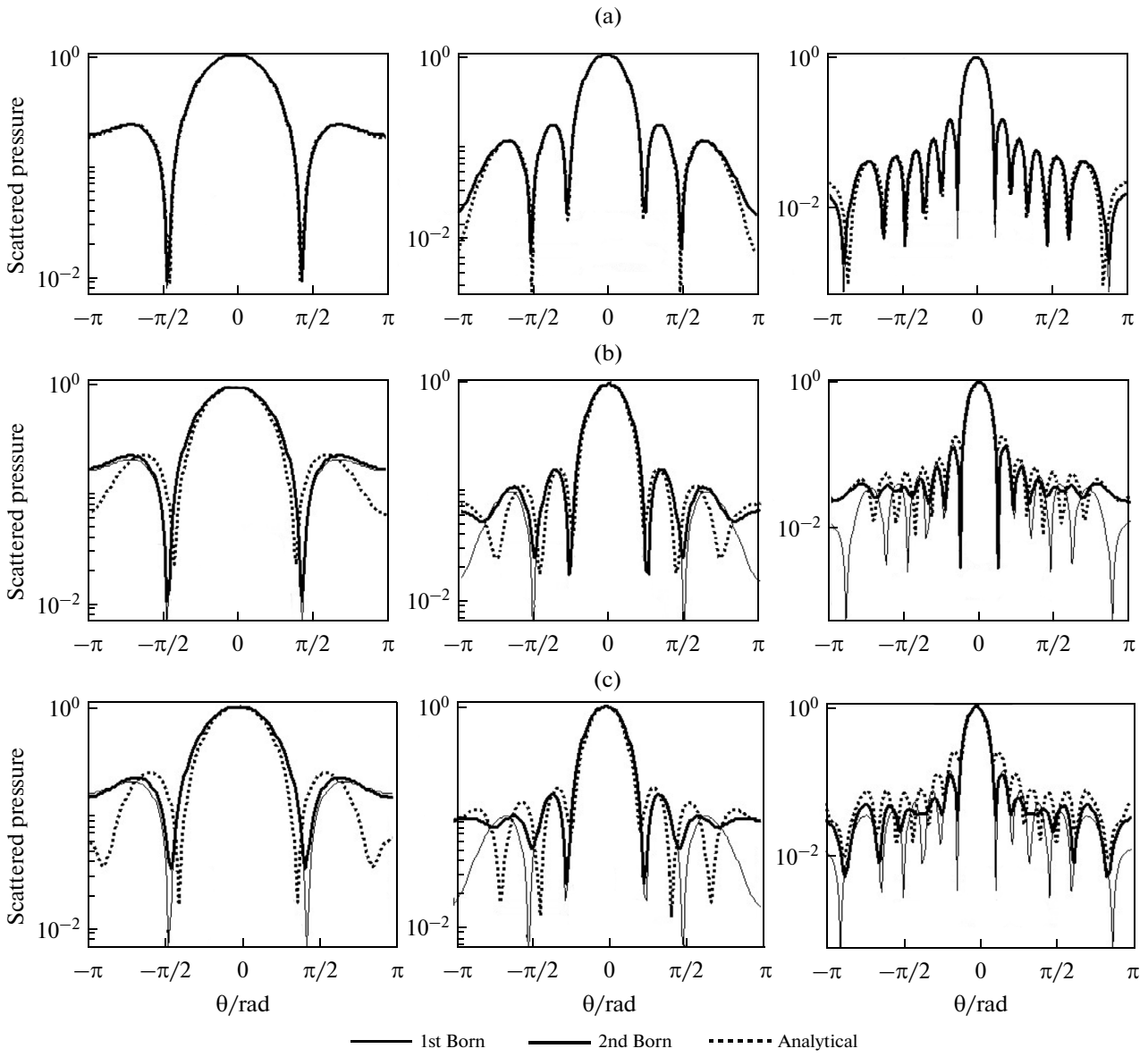

Fig. 5. Directional patterns of sound waves scattered from cylinder softer than water: (a) $D = 0.99$ and $S = 0.99$, with $k_0R = 3$, 5 and 10 from left to right; (b) $D = 0.90$ and $S = 0.90$, with $k_0R = 3$, 5 and 10 from left to right; (c) $D = 0.85$ and $S = 0.85$, with $k_0R = 3$, 5 and 10 from left to right.

incident sources, and using the same transform-domain sampling technique as in the first-order case, Kak's proposition of higher-order solution by iteration is conveniently implemented. The obtained correction term is added to the first-order solution, leading to better prediction of sound scattering. It has been shown that the prediction accuracy is improved, and the range of applicable ρc ratios has effectively exceeded the weak scattering limitation. For example, based on the first-order approximation, sound scattering from squid with the ρc ratio less than 1.1 was studied in [12]. Using the second-order approximation in the FDT-based approach proposed in this paper, the applicable range of the ρc ratio is at least 0.72–1.44 when $k_0R < 10$.

It should be noted that, even with the second-order approximation, the method will still not work for strong scatterers. Introduction of third-order correction increases computation time significantly with little advantage as compared to the second-order results. Therefore further research is required for more improvements. Also, shear waves in the object need to be considered to make the FDT-based approach applicable to a wider scope of applications.

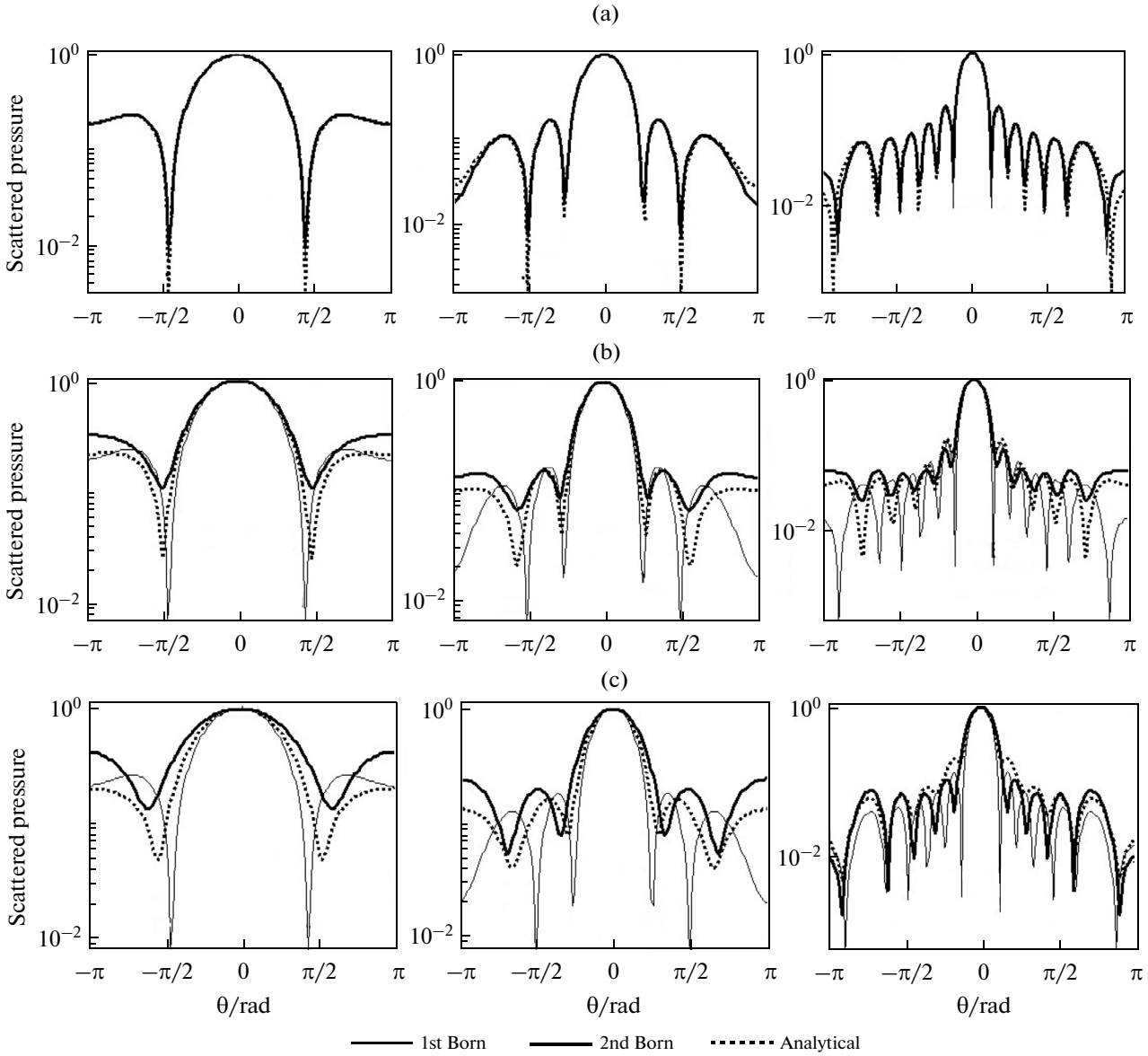

Fig. 6. Directional patterns of sound waves scattered from cylinder harder than water: (a) $D = 1.01$ and $S = 1.01$, with $k_0R = 3$, 5 and 10 from left to right; (b) $D = 1.10$ and $S = 1.10$, with $k_0R = 3$, 5 and 10 from left to right; (c) $D = 1.20$ and $S = 1.20$, with $k_0R = 3$, 5 and 10 from left to right.

ACKNOWLEDGMENTS

This work was supported by the Natural Science Foundation of China under grant no. 61071187 and the Public Science and Technology Research Projects of Ocean Engineering (201305019).

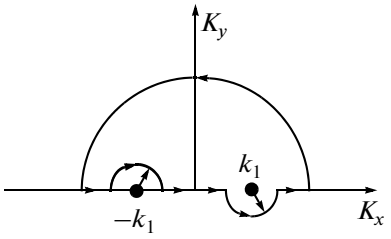

Fig. A. Contour integral.

REFERENCES

1. Yu. A. Kobelev, Acoust. Phys. **57**, 447 (2011).
2. V. C. Anderson, J. Acoust. Soc. Am. **22**, 426 (1950).
3. S. J. Bezuszka, J. Acoust. Soc. Am. **26**, 148 (1954).
4. M. B. Salin, E.M. Sokov, and A.S. Suvorov, Acoust. Phys. **57**, 722 (2011).
5. M. Zampolli, F. B. Jensen, and A. Tesei, J. Acoust. Soc. Am. **125**, 89 (2009).
6. S. Wang, J. Acoust. Soc. Am. **99**, Pt. 1, 1924 (1996).
7. M. M. Shabat, N. M. Barakat, S. Al-Azab, and D. Jager, in Proc. SPIE **4829**, 251 (2003).

8. P. S. Naidu, A. Vasuki, P. Satyamurthy, and L. Anand, IEEE Trans. on Ultrason., Ferroelect. Freq. Cont. **42**, 787 (1995).
9. S. Wang, in *Proc. 17th Int. Congress on Sound and Vibration, Cairo, Egypt, 2010.*
10. P. Zhang, S. Wang, R. Wang, Y. Chen, and L. Wang, J. Acoust. Soc. Am. **131**, Pt. 2, 3485 (2012).
11. K. Iwata and R. Nagata, Jap. Soc. Appl. Phys. **14**, 379 (1975).
12. B. A. Jones, A. C. Lavery, and T. K. Stanton, J. Acoust. Soc. Am. **125**, 73 (2009).
13. R. K. Saha and S. K. Sharmëa, Phys. Med. Biol. **50**, 2823 (2005).ì
14. Z. Lu and U. Zhang, IEEE Trans. Ultrason., Ferroelect., Freq. Cont. **43**, 296 (1996).
15. A. C. Kak and M. Slaney, in *Principles of Computerized Tomographic Imaging* (IEEE, New York, 1999), pp. 220–273.
16. A. J. Devaney, J. Acoust. Soc. Am. **78**, 120 (1985).
17. D. Chu and Z. Ye, J. Acoust. Soc. Am. **106**, Pt. 1, 1732 (1999).
18. P. Zhang, S. Wang, and R. Wang, J. Visual Commun. Image Represent. **23**, 697 (2012).
19. L. Tian and X. Hu, J. Shanxi Norm. Univ. (Natural Science Edition) **22**, 54 (2008) [in Chinese].

APPENDIX

Here we give derivation of (17)–(19), the directional pattern of the second-order correction contributed by the first-order scattering in the direction $\theta^{[1]}$. As discussed in Section 3, by substituting the first-order scattered wave into (13), the second-order correction to the first-order scattered wave (15) is

$$p_s^{[2]}(\mathbf{r}) = \int o(\mathbf{r}')\{\int[k_0^2\gamma_\kappa o(\mathbf{r}'')p_i(\mathbf{r}'')g(\mathbf{r}'|\mathbf{r}'') + \gamma_\rho o(\mathbf{r}'')\nabla p_i(\mathbf{r}'')\cdot\nabla g(\mathbf{r}'|\mathbf{r}'')]d\mathbf{r}''\}g(\mathbf{r}|\mathbf{r}')d\mathbf{r}'. \quad \text{(A1)}$$

The exponential term in the secondary incidence is $\exp[jk_0(1+\alpha)x] = \exp(jk_1x)$ [12, 17], and the Green's functions are

$$g(\mathbf{r}|\mathbf{r}') = \sqrt{\frac{2}{\pi r}}\exp[-jk_0(x'\cos\theta^{[2]} + y'\sin\theta^{[2]})] \times \exp\left(jk_0r - j\frac{\pi}{4}\right). \quad \text{(A2)}$$

Here, plane wave expansion of $g(\mathbf{r}'|\mathbf{r}'')$ is [19]

$$g(\mathbf{r}'|\mathbf{r}'') = \frac{j}{4\pi}\int\!\!\int\frac{1}{k_1^2 - K^2}\exp[j\mathbf{K}\cdot(\mathbf{r}' - \mathbf{r}'')](dK_x)dK_y = \frac{j}{4\pi}\oint\frac{K}{k_1^2 - K^2}\exp[jK(x'\cos\theta^{[1]} - x''\cos\theta^{[1]}) + jK(y'\cos\theta^{[1]} - y''\sin\theta^{[1]})]dK, \quad \text{(A3)}$$

where $K^2 = K_x^2 + K_y^2$. Thus the first term in (A1) can be expanded as follows:

$$k_0^2\gamma_\kappa\int o(\mathbf{r}')\{\int[o(\mathbf{r}'')p_i(\mathbf{r}'')g(\mathbf{r}'|\mathbf{r}'')]d\mathbf{r}''\}g(\mathbf{r}|\mathbf{r}')d\mathbf{r}' = \frac{j}{4\pi}\sqrt{\frac{2}{\pi r}}\exp\left(jk_0r - j\frac{\pi}{4}\right)k_0^2\gamma_\kappa \times\oint\frac{KO(k_1\cos\theta^{[2]} - K\cos\theta^{[1]},\, k_1\sin\theta^{[2]} - K\sin\theta^{[1]})O(K\cos\theta^{[1]} - k_1, K\sin\theta^{[1]})}{k_1^2 - K^2}dK. \quad \text{(A4)}$$

Since scattering is outgoing, the contour goes above the pole $K = -k_1$ and below $K = +k_1$, as shown in Fig. A. Thus, there is only one pole inside the contour, and the integral in (A4) can be worked out using the residue theorem:

$$\oint\frac{KO(k_1\cos\theta^{[2]} - K\cos\theta^{[1]},\, k_1\sin\theta^{[2]} - K\sin\theta^{[1]})O(K\cos\theta^{[1]} - k_1, K\sin\theta^{[1]})}{k_1^2 - K^2}dK = \frac{1}{2}O(k_1\cos\theta^{[2]} - k_1\cos\theta^{[1]},\, k_1\sin\theta^{[2]} - k_1\sin\theta^{[1]})O(k_1\cos\theta^{[1]} - k_1,\, k_1\sin\theta^{[1]}). \quad \text{(A5)}$$

Since

$$\nabla p_i(\mathbf{r}'')\cdot\nabla g(\mathbf{r}'|\mathbf{r}'') = k_1^2(\cos\varphi, \sin\varphi)(\cos\theta^{[1]}, \sin\theta^{[1]}) \times p_1(\mathbf{r}'|\mathbf{r}'') = k_1^2\cos(\varphi - \theta^{[1]})p_i(\mathbf{r}'')g(\mathbf{r}'|\mathbf{r}'') = k_1^2\cos(\theta^{[1]})p_i(\mathbf{r}'')g(\mathbf{r}'|\mathbf{r}''), \quad \text{(A6)}$$

with $\varphi = 0$, the dot products of two gradients in the second term of (A1) can be simplified:

$$\gamma_\rho\int\{o(\mathbf{r}')(\int[o(\mathbf{r}'')\nabla p_i(\mathbf{r}'')\cdot\nabla g(\mathbf{r}'|\mathbf{r}'')]d\mathbf{r}'')g(\mathbf{r}|\mathbf{r}')\}d\mathbf{r} = \gamma_\rho k_1^2\cos\theta^{[1]}\int\{o(\mathbf{r}')(\int[o(\mathbf{r}'')p_i(\mathbf{r}'')g(\mathbf{r}'|\mathbf{r}'')]d\mathbf{r}'') \times g(\mathbf{r}|\mathbf{r}')\}d\mathbf{r}'. \quad \text{(A7)}$$

Therefore, the contribution of the first-order scattering in the direction $\theta^{[1]}$ to the directional pattern of the second-order increment is obtained by combining (A4), (A5) and (A7):

$$f(\theta^{[1]}, \theta^{[2]}) = (k_0^2\gamma_\kappa + \gamma_\rho k_1^2\cos\theta^{[1]}) \times (k_1\cos\theta^{[2]} - k_1\cos\theta^{[1]},\, k_1\sin\theta^{[2]} - k_1\sin\theta^{[1]}) \times O(k_1\cos\theta^{[1]} - k_1,\, k_1\sin\theta^{[1]}). \quad \text{(A8)}$$